JOURNAL OF MATERIALS SCIENCE 29 (1994) 2663–2670

Non-equilibrium segregation of solutes to grain boundary

Part III *Mechanism of non-equilibrium segregation*

SANHONG ZHANG, XINLAI HE, T. KO
Department of Materials Physics, University of Science and Technology Beijing, Beijing 100083, P. R. China

Mechanisms for the non-equilibrium segregation of solutes to static grain boundary during cooling (quenching-induced segregation) and to moving grain boundary during recrystallization (moving-induced segregation) are proposed. For quenching-induced segregation, in consideration of the local equilibrium among vacancies, solute atoms and vacancy-solute atom complexes, as well as the influence of equilibrium grain-boundary segregation, the theoretical dynamic formulae for this non-equilibrium segregation have been derived on the basis of the vacancy-dragging mechanism. Theoretical calculations have been carried out for the non-equilibrium segregation of boron to austenitic grain boundaries during isothermal holding and continuous cooling after heating at high temperature; the results agree well with those obtained from experiments. The model has also successfully explained the different behaviours of boron segregation during cooling in α-Fe and in γ-Fe. For moving-induced segregation, based on the interaction between dislocations and the moving boundaries during recrystallization, a dislocation relaxation and widening grain-boundary mechanism of solute segregation on moving boundaries is proposed. Applying this model, we have calculated the boron segregation on moving boundaries during recrystallization in Fe–3% Si alloy; the results of these calculations agree with experimental results.

1. Introduction

It is known that quenching, strain, radiation and recrystallization can induce non-equilibrium segregation of solutes to surface and interface. For example, quenching-induced non-equilibrium segregation has been described for boron in γ-Fe, Ti and Au in Pb alloy as well as solute in ZnAl alloy and SnPb alloy [1–3]. Strain-induced non-equilibrium segregation of boron to grain boundaries is seen in γ-Fe [4]. Electron radiation-induced non-equilibrium segregation is seen in Cu in Ni–2% Cu alloy, and Si in Cu–2% Si alloy [5]. Recently, an unusual distribution of solute on moving grain boundaries or recrystallized boundaries has been reported [4, 6].

Quenching- and strain-induced segregation have been attributed to diffusion of vacancy–solute complexes along vacancy gradients to the grain boundary, the diffusion resulting from the super-saturation vacancies (produced with quenching or deformation) annihilated at grain boundaries — a vacancy–solute complex (or vacancy-dragging) mechanism [3]. It is thought that the occurrence of radiation-induced segregation resulted in the annihilation of point defects (vacancies, interstitials and small defect clusters) at sinks. Vacancy–solute complex diffusion, interstitial–solute complex diffusion and inverse Kirkendall effects were thought to be the main mechanisms leading to radiation-induced segregation. Concerning the mechanism of moving-induced segregation, few theoretical studies have been undertaken.

The aims of this work are as follows. (i) The vacancy–solute complex mechanism of non-equilibrium segregation is investigated further, and general diffusion equations involving vacancy, solute and complex diffusion are obtained. (ii) The behaviour of the recrystallized grain boundary is also studied, and a mechanism for the non-equilibrium segregation of solute atoms on the moving boundary is proposed. (iii) The two models are applied to the following two systems: non-equilibrium segregation of boron to grain boundaries during cooling in γ-Fe [1, 7]; and boron segregation on moving grain boundaries during recrystallization after deformation at 1000 °C in Fe–3% Si alloy.

2. Vacancy–solute complex mechanism

2.1. Model

Quenching, deformation and radiation can produce non-equilibrium vacancies. If $E_b > kT$ (where E_b is the binding energy of vacancy and solute atom), there exist stable vacancy–solute complexes in crystals. The complex diffusion to the grain boundary, along with the supersaturation vacancy annihilation at the grain boundary, can induce non-equilibrium segregation of

0022–2461

solute to grain boundary. Here we study quenching-induced non-equilibrium. At a temperature T, there exists a certain equilibrium concentration of free vacancy C_V^{eq} in a crystal given by

$$C_V^{eq} = K_V \exp(E_V/kT) \tag{1}$$

where E_V is the formation energy of a vacancy and K_V is the entropy term. For a binary alloy system, vacancy(V)–solute(B) complexes (VB) will be formed by the equilibrium reaction $V + B = VB$. The complex equilibrium concentration C_{VB} is

$$C_{VB} = K_0 C_V C_B \exp(E_b/kT) \tag{2}$$

where C_V and C_B are concentrations of vacancy and solute, respectively, E_b is the binding energy of solute and vacancy, and K_0 is a constant. The total solute concentration in alloy is $C_B + C_{VB}$. As shown in Fig. 1a, at a high temperature T_1 the concentrations of species V, B and VB in crystal are homogeneously distributed at equilibrium levels. When the alloy is quenched to and isothermally held at a relatively low temperature T (Fig. 1b), the supersaturated vacancies will be annihilated at grain boundaries, causing the decomposition of complex there. Thus along with the vacancy gradient a complex gradient is developed, and the complexes move to grain boundaries, enriching the solute there. In the meantime a solute gradient is set up at the opposite direction of the complex gradient, the free solute will diffuse away from grain boundaries in a back-diffusion process. Non-equilibrium segregation on grain boundaries will arise if the solute enrichment process dominates the back-diffusion process. With the prolongation of the isothermal holding time at temperature T, the segregation increases at first due to the annihilation of supersaturated vacancies, and then decreases when the back-diffusion process becomes dominant.

It is suggested that in the process of non-equilibrium segregation the changes in concentrations of V, B and VB in a local region result not only from the diffusion of these species driven by their concentration gradients, but also from the complex formation and decomposition reactions to keep the equilibrium among these species in this region. Supposing F is the rate of complex decomposition, according to Fick's Second Law and conservation of matter, we find:

$$\begin{aligned} \frac{\partial C_{VB}}{\partial t} - D_{VB}\nabla^2 C_{VB} &= -F \\ \frac{\partial C_V}{\partial t} - D_V \nabla^2 C_V &= F \\ \frac{\partial C_B}{\partial t} - D_B \nabla^2 C_B &= F \end{aligned} \tag{3}$$

where D_V, D_B and D_{VB} are diffusion coefficients of vacancy, solute and complex, respectively.

According to the literature [8], the rate (F) of complex concentration change resulting from the reaction $V + B = VB$ of the three species at local region is

$$F = (R_1 D_V + R_2 D_B)\left(C_B C_V - \frac{C_{VB}}{K}\right)$$

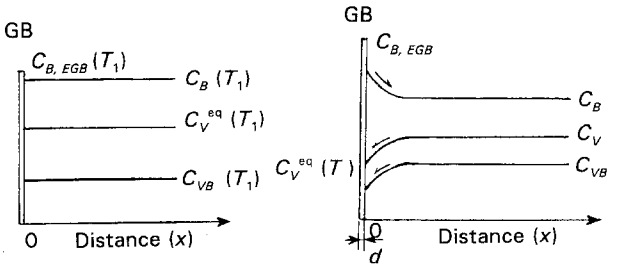

Figure 1 Schematic drawing of concentration distribution of vacancy, solute and vacancy–solute complex near grain boundary (GB). (a) At temperature T_1; (b) quenched to and held at temperature T.

where $K = K_0 \exp(E_b/kT)$, and R_1 and R_2 are constants relating to the properties and configuration of the complex.

Substituting F into Equation 3, we obtain

$$\frac{\partial C_B}{\partial t} = D_B \nabla^2 C_B - (R_1 D_V + R_2 D_B) \times \left(C_B C_V - \frac{C_{VB}}{K}\right) \tag{4}$$

$$\frac{\partial C_V}{\partial t} = D_V \nabla^2 C_V - (R_1 D_V + R_2 D_B) \times \left(C_B C_V - \frac{C_{VB}}{K}\right) \tag{5}$$

$$\frac{\partial C_{VB}}{\partial t} = D_{VB} \nabla^2 C_{VB} + (R_1 D_V + R_2 D_B) \times \left(C_B C_V - \frac{C_{VB}}{K}\right) \tag{6}$$

Equations 4–6 are the general forms of vacancy and interstitial atom diffusion equations. It is found that the diffusion process of vacancy and interstitial are coupled through a complex reaction. When the binding between interstitial and vacancy is very weak, there are no thermal stable complexes in the crystal. Thus the complex cannot be treated as a diffusion unit. In this case, $K = K_0 = Z$ (Z is the number of the nearest atoms), $C_{VB} = Z C_V C_B$. Substituting these two equations into Equations 4 and 5, Equations 4 and 5 become the diffusion equations in Fick's Second Law. When the binding is strong, the effect of complexes cannot be neglected, and the diffusion of three species is coupled through a complex reaction. The degree of influence is determined by the binding energy E_b and the rate of complex change F. In the extreme case, the rate of complex formation and dissociation is so fast, the reaction $V + B = VB$ can always maintain local equilibrium. Of course, in practical diffusion processes, this reaction can not maintain equilibrium absolutely. But if the time of the reaction reaching equilibrium is much less than the diffusion time in the overall system, it is reasonable to consider that the reaction always maintains local equilibrium in the process of diffusion. In this case, Equations 4–6 become Equations 7–9

$$\frac{\partial C_B}{\partial t} + \frac{\partial C_{VB}}{\partial t} = D_B \nabla^2 C_B + D_{VB} \nabla^2 C_{VB} \tag{7}$$

$$\frac{\partial C_V}{\partial t} + \frac{C_{VB}}{\partial t} = D_V \nabla^2 C_V + D_{VB} \nabla^2 C_{VB} \quad (8)$$

$$C_{VB} = K C_V C_B \quad (9)$$

2.2. Calculation of quenching-induced segregation of boron in γ-Fe

Equations 7–9 can be applied to calculate the quenching-induced non-equilibrium segregation of boron to grain boundary in γ-Fe. According to Karlsson [9], for boron in γ-Fe the time of the reaction $V + B = VB$ to reach the equilibrium state is

$$\Delta t_0 = \frac{B\left(\frac{V_a}{C_V}\frac{V_a}{C_B}\right)^{1/2}}{(D_V D_B)^{1/2}}$$

where V_a is the atomic volume in the crystal. Thus Equations 7 and 8 can be used to describe the boron non-equilibrium segregation in γ-Fe with the condition that the Δt_0 is a negligible quantity compared with the time of the whole diffusion process. In practical calculation through the finite difference method, this condition is that the time increment Δt must be larger than Δt_0. In the present work, this condition can be met for the calculation of boron segregation at austenite grain boundaries above 600 °C.

For a specimen heated at a temperature T_1, then quenched to and isothermally held at a temperature T, the boundary and initial conditions for the calculation are given as follows (see Fig. 1).

(i) The vacancy concentration in the region close to grain boundaries is always kept at its thermal equilibrium value $C_V^{eq}(T)$ determined by Equation 1 at temperature T; that is, $C_V|_{X=0} = C_V^{eq}(T)$.

(ii) Taking account of the equilibrium grain-boundary segregation, the solute concentration at grain boundaries ($C_{B,\,EGB}$ in Fig. 1) can be expressed as $\alpha \cdot (C_B + C_{VB})|_{X=0}$, where α is the equilibrium segregation factor of the solute and is a function of temperature. Assuming the width of the grain boundary (d) is very narrow, taken as 1.0 nm in the following calculation, we find

$$(d/2)\frac{\partial \alpha (C_B + C_{VB})|_{X=0}}{\partial t} = (D_B C_B + D_{VB} C_{VB})|_{X=0} \quad (10)$$

(iii) Homogeneous distribution of the three species in the matrix is considered as an initial condition. The total vacancy concentration ($C_V + C_{VB}$), as well as the total solute concentration ($C_B + C_{VB}$) are equal to the values at T_1. Using the equilibrium relation of Equation 2 at T, the initial values of C_V, C_B and C_{VB} can be obtained.

According to the mechanism suggested above, the segregation of boron to austenite grain boundaries is calculated using a computer. The parameters used are

D_V ($m^2\,s^{-1}$) [10, 11]	$1.4 \times 10^{-5} \exp(1.4/kT)$
D_B ($m^2\,s^{-1}$) [12]	$2 \times 10^{-7} \exp(-1.15/kT)$
D_{VB} ($m^2\,s^{-1}$) [13, 14]	$2 \times 10^{-6} \exp(-1.15/kT)$
C_V^{eq} [14, 15]	$4.5 \exp(-1.4/kT)$
E_b (eV) [13, 16]	0.5
K_0 [9, 17]	4
α [18]	$\exp(0.42/kT)$
d (nm) [19]	1

The initial total B concentration is 20 p.p.m. and the grain size is 40 μm.

A finite-difference method is used for the numerical calculation, in which the increment of the distance (x) from a grain boundary is

$$\Delta X = 0.25\ \mu m\ (\geqslant 720\,^\circ C);\quad 0.07\ \mu m\ (< 720\,^\circ C)$$

To ensure the convergence of solution, the time increment is given by

$$\Delta t = \frac{(\Delta X)^2}{2 \times \max(D_V D_B D_{VB})}$$

In order to make comparisons with the experimental results by particle-tracking autoradiography (PTA), the enrichment factor of grain-boundary segregation is defined as $I = (C_{gb} - C_g)/C_g$, where C_{gb} is the total solute concentration at a grain boundary region, which includes the grain boundary *per se* and the area with 2.5 μm width adjacent to it. The C_g is that interior to the grain. For simplicity, as the temperature is below 630 °C, the diffusion process is neglected in the calculation as the diffusion species concerned can hardly move at those temperatures. Thus, if the heated temperature is lower than 630 °C the segregation in the specimen cooled to room temperature is same as that at the heated temperature. The calculation results are detailed below.

2.2.1. Boron segregation during isothermal holding

The grain boundary segregation of B as a function of isothermal holding time at 1000 °C after quenching from 1200°C has been calculated (shown in Fig. 2a), which can be compared with the experimental result measured by PTA (Fig. 2b [7]). It is found that with the prolongation of isothermal holding time, the segregation intensifies to a maximum and then declines. The peaks appear at about 3 s on both the calculation and experimental curves.

2.2.2. Relationship between segregation and cooling rate during continual cooling

The calculation result for the grain-boundary segregation of B varied with cooling rate is given in Fig. 3, which shows that after heating at 1000 °C, as the cooling rate reduces the segregation increases, but then decreases at relatively lower cooling rates, and a maximum appears at about 10 °C s^{-1}. In fact, by means of secondary ion mass spectrum (SIMS) and atom probe (AP), Karlsson *et al.* [20] found that the strongest enrichment occurs at intermediate cooling rates (around 13 °C s^{-1}) for 316L austenitic stainless steels.

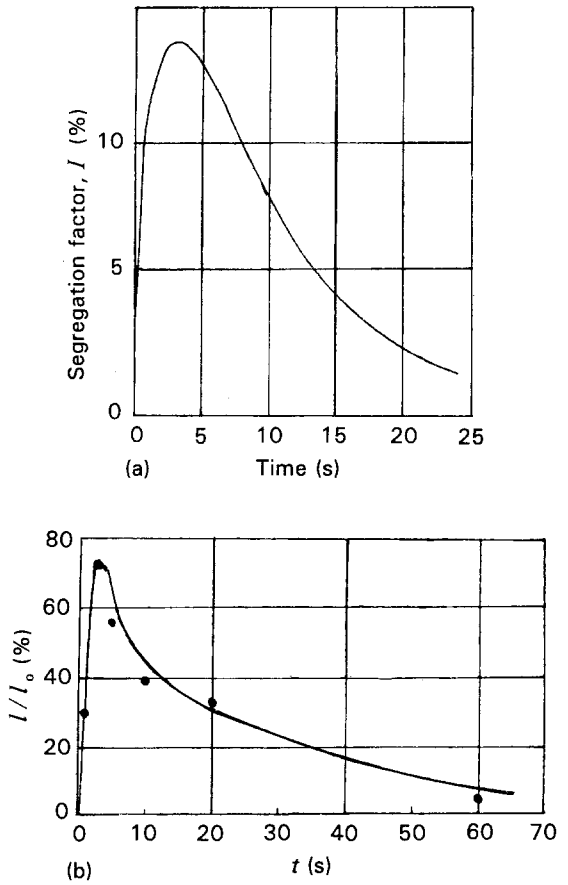

Figure 2 Boron segregation at austenite grain boundary as a function of isothermal holding time at 1000 °C after quenching from 1200 °C. (a) calculation result; (b) experimental result.

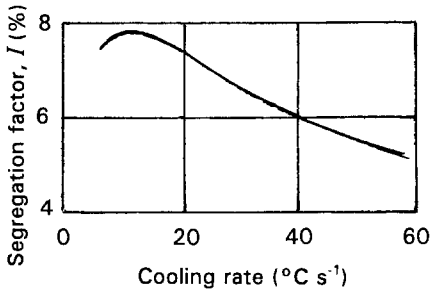

Figure 3 Calculation of boron segregation at austenite grain boundary as a function of cooling rate after heating at 1000 °C.

2.2.3. Boron segregation after quenching from different temperatures

The influence of heating temperature on the grain boundary segregation of B in a continuous cooling test has been experimentally measured in Fe–30% Ni alloys (shown in Fig. 4b [9]), and the corresponding calculation result is given in Fig. 4a. Both results show that at usual cooling rates there exists a minimum segregation at a certain quenching temperature, referred to as the transition temperature. The equilibrium or non-equilibrium segregation is dominant when the quenching temperature is below or beyond the transition temperature, respectively. Contrary to the equilibrium segregation, the non-equilibrium segregation is enhanced as the quenching temperature is increased. The non-equilibrium segregation formed during cooling is sensitive to the cooling rate. The

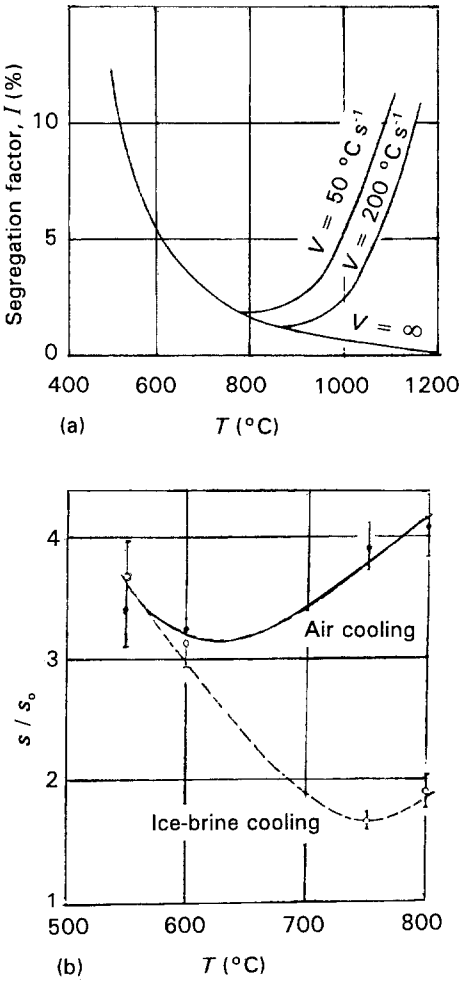

Figure 4 Boron segregation at austenite boundary as a function of quenching temperature at different cooling rates. (a) Calculation result; (b) experimental result.

transition temperature goes up as the cooling rate increases, and at an infinitely high cooling rate the non-equilibrium segregation will be completely inhibited and the segregation exclusively dependent on the equilibrium segregation formed during heating.

A good fit of the theoretical calculations to the experimental results demonstrated the aptness of the model. As the equilibrium segregation has been considered in the boundary conditions (Equation 10), the segregation behaviour including equilibrium and non-equilibrium segregation is comprehensively described by these dynamic equations (Equations 7–9).

2.3. Discussion

It can be seen that in this model $D_{VB} > D_B$ and $E_b > kT$ are necessary conditions for the occurrence of the non-equilibrium segregation induced by quenching. The experimental results, which show that there is non-equilibrium segregation of boron to grain boundaries in γ-Fe but not in α-Fe [21, 22], may be explained with this model. The diffusivity of boron and vacancy in α-Fe [12, 21] is shown in Fig. 5. It can be seen that boron diffusivity is greater than vacancies in the experimental temperature range used in [22]. Thus it is difficult to imagine that the complex (boron and vacancy) diffusivity will be greater than that of

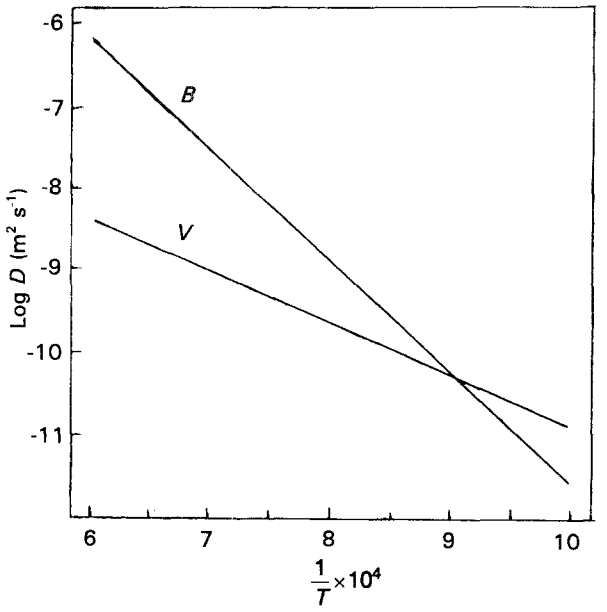

Figure 5 Diffusivity against $1/T$ (K) for boron and vacancy in α-Fe. $D_V = 2.45 \times 10^{-5} \exp(-1.24/kT)$; $D_B = 100\exp(-2.67/kT)$.

boron. On the other hand, according to the theoretical calculation [21], the binding energy between boron and vacancy E_b in α-Fe is less than 0.091 eV, which is much less than E_b (0.51 eV) [13, 16] in γ-Fe. According to the above model, we can expect that there is no boron non-equilibrium segregation to grain boundaries in α-Fe, and the experimental results prove this point.

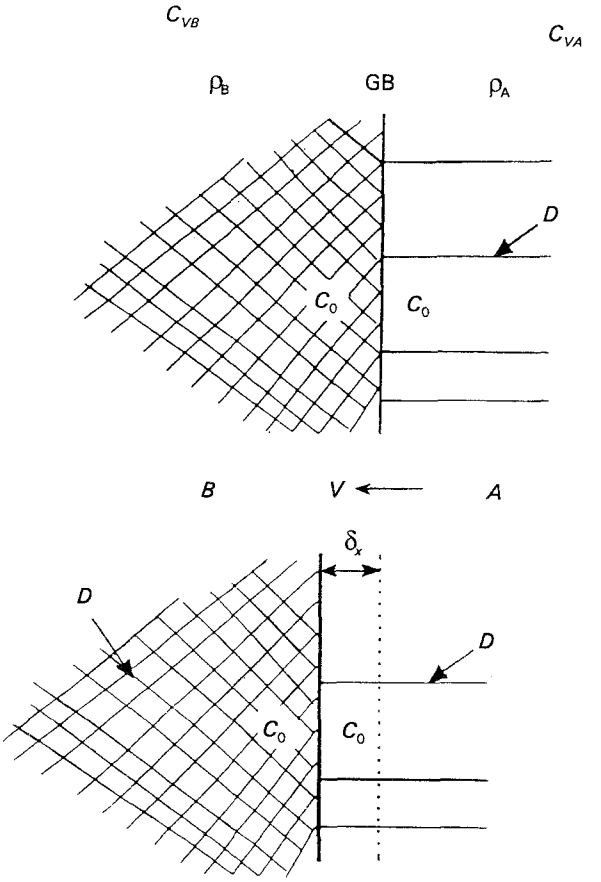

Figure 6 Schematic diagram of boundary migration during recrystallization. $\rho_B \gg \rho_A$. ρ_A, dislocation density in region A; ρ_B, dislocation density in region B; D, Dislocation; C_0, boron concentration in the matrix; C_{VA}, vacancy concentration in region A; C_{VB}, vacancy concentration in region B.

3. Mechanism of non-equilibrium segregation of solute to moving grain boundary during recrystallization

3.1. Model

It has been shown that the segregation of boron at moving grain boundary during recrystallization in Fe–3% Si is stronger than the segregation on static grain boundary at the same temperature [23]. This type of solute segregation on the moving boundary cannot have been properly interpreted by the existing theories of solute segregation to moving boundaries. According to the solute drag theory of Cahn [24], the solute segregation on moving boundaries is not higher than the equilibrium segregation estimated by McLean's equation [25] at the same temperature.

A relaxation mechanism of dislocation disappearing in moving boundaries seems able to account for this perversive segregation. During the recrystallization process, the new grain boundaries will move toward the high dislocation density (ρ_A) areas, and leave regions with low dislocation density (ρ_B) behind them (Fig. 6). This means that a large number of dislocations will be annihilated in the moving boundaries during recrystallization. The experimental results [26] have indicated that the process of dislocation annihilation in grain boundaries (Fig. 7) need an appreciable time (relaxation time, τ). During this time τ, the dislocation incorporated in a boundary will give the boundary an extra distortion area at the position where the dislocation enters, and the local boundary thickness will increase (Fig. 7 illustrates a lattice dislocation annihilation in a grain boundary). The increase in the moving boundary width leads to a bigger area that solute atoms can segregate to.

Fig. 8 illustrates solute atom free energy and diffusion coefficient distribution across the moving boundary. In Fig. 8, δ is the width of the moving grain boundary, and $U_0 = F_g - F_{gb}$ is the binding energy of solute segregation to grain boundary. D_g and D_{gb} are the diffusion coefficient of solute in grain boundaries and interior grains, respectively.

Assuming that a length of dislocation entering into boundary leads an increment (d_τ) of average width of unity area boundary during τ, then the width of the moving boundary, δ, is

$$\delta = d_0 + (\rho_B - \rho_A) V \tau d_\tau$$

where V is the boundary velocity, d_0 is the static boundary width, and ρ_B and ρ_A are the dislocation density in deformed grains and new grains, respectively. Because $\rho_B \gg \rho_A$ ($\rho_B \equiv \rho$),

$$\delta = d_0 + \rho V \tau d_\tau$$

However, the increasing width does not necessarily mean an increase of segregation. As in Cahn's theory [24] (note: in Cahn's treatment the width of moving boundary is same as the static boundary) the solute

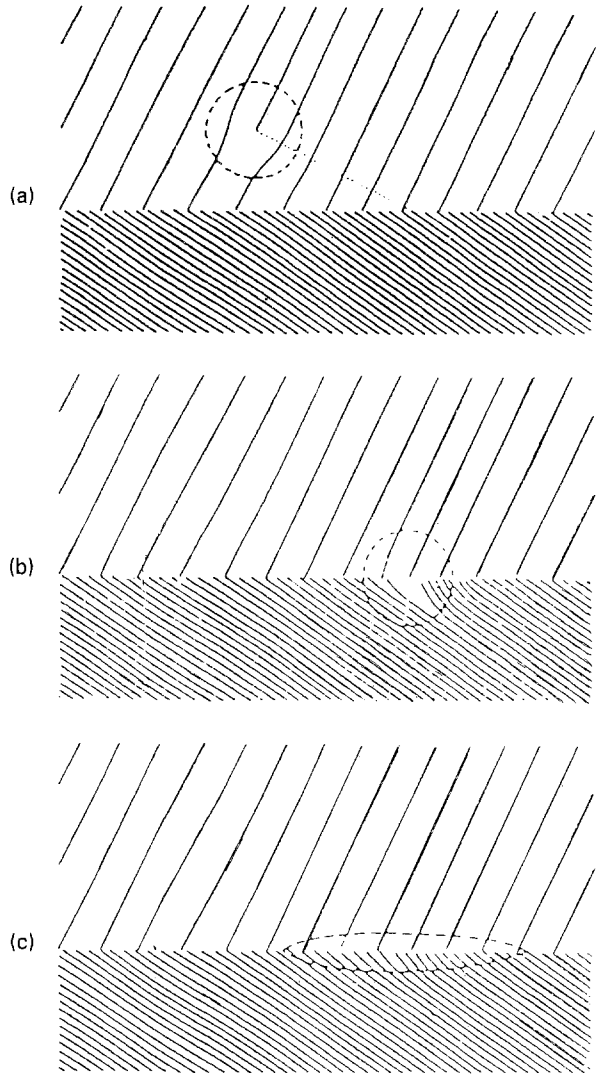

Figure 7 Schematic diagram to illustrate the model of dislocation delocalization in a grain boundary [37].

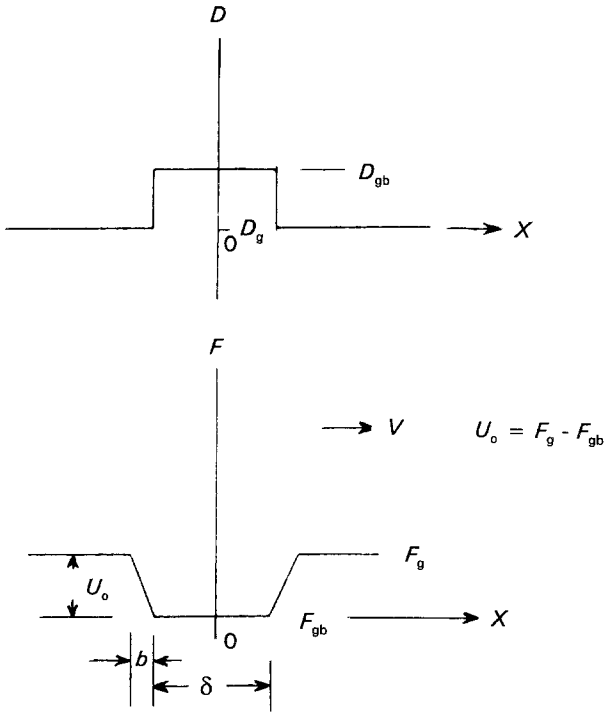

Figure 8 Diffusion coefficient and potential of solute atom near and at grain boundary.

distribution across the moving boundary of Fig. 8 is shown in Fig. 9.

In order to compare with the experimental result [23] which is the ratio of average solute concentration in the boundary area of W (W = 6.42 μm [23]) width to the concentration in grain, we calculated the average concentration C_{gb} of solute in the boundary area of W ($\delta < W$) [21, 24]. Assuming $b/\delta \ll 1$, then

$$C_{gb} = C_0 + \frac{C_0 D_{gb}}{WV}\left(e^{\frac{U_0}{kT}} - \frac{Vb}{D_{gb}} - 1\right) \times \left(1 - \frac{1}{1 - \frac{U_0 D_g}{VbkT}}\right)(1 - e^{-V\delta/D_{gb}}) \tag{11}$$

For $U_0 > kT$ (which means that the solute atoms have a considerable equilibrium segregation on the static boundary), and assuming b is a small quantity, then Equation 11 is simplified to

$$\frac{C_{gb}}{C_g} = 1 + \frac{D_{gb}}{WV}\left(e^{\frac{U_0}{kT}} - 1\right)\left(1 - e^{-\frac{V\delta}{D_{gb}}}\right) \tag{12}$$

It can be seen that when $V \to \infty$, $C_{gb}/C_0 \to 1$, it means there is no segregation on the moving boundary with high velocity. When $V \to 0$,

$$\frac{C_{gb}}{C_g} = 1 + \frac{1}{W}\left(e^{\frac{U_0}{kT}} - 1\right)d_0 \quad (V = 0 \to \delta = d_0)$$

which is the equilibrium segregation value of solute on static boundaries. From Equation 12 we can find that when $D_{gb} \gg V\delta$ there is a strong segregation on the moving boundary, even stronger than the equilibrium segregation on static boundaries. $D_{gb} \gg V\delta$, Equation 12 becomes

$$\frac{C_{gb}}{C_g} = 1 + \frac{1}{W}\left(e^{\frac{U_0}{kT}} - 1\right)\delta$$

$$\delta = d_0 + \rho V \tau d_\tau$$

$$\frac{C_{gb}}{C_g} = 1 + \frac{1}{W}\left(e^{\frac{U_0}{kT}} - 1\right)(d_0 + \rho V \tau d_\tau) \tag{13}$$

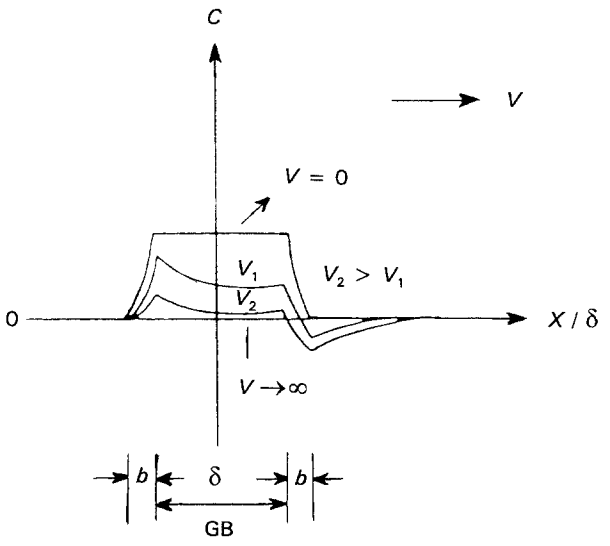

Figure 9 Schematic diagram of concentration profiles for four migration rates.

$D_{gb} \gg V\delta$, which means that the solute atoms can follow moving boundaries as an atmosphere (otherwise the moving boundaries will break away from the solute atmosphere). As the boundary width is increased (i.e. V is increased) there are more solute atoms moving along with the moving boundary, then the solute segregation becomes strong.

3.2. Applications

Equation 13 is applied to calculate the boron segregation on moving grain boundaries in Fe–3% Si during recrystallization at 1000 °C. In the case of equilibrium segregation of boron on static grain boundaries at 1000 °C, the enrichment ratio (K^{eq}) of the average boron concentration in the boundary area of 6.42 μm width (W) to the boron concentration interior grain is [22]

$$K^{eq} = 1 + [d_0/W] * [\exp(U_0/kT) - 1] = 1.1 \quad (14)$$

From the above equation and Equation 13, it can be found that the enrichment ratio C_{gb}/C_g (K^{MG}) on the moving boundaries can be easily obtained once δ is known. $\delta (= d_0 + \rho V \tau d_\tau)$ is calculated as follows.

(i) The bulk density ρ of dislocation in deformed grain is about 1.5×10^{11} cm^{-2} [27].

(ii) The boundary velocity is $\sim 2.8 \times 10^{-4}$ cm s^{-1} [27].

(iii) The dislocation core region is suggested to be the same as the boundary region for solute segregation. r_0 is the radius of the dislocation core region. During the process of extrinsic dislocation (unit length) annihilation at moving boundary, the increasing width of the unit area boundary, d_τ, can be obtained from the following equation

$$d_\tau * 1 \text{ cm} * 1 \text{ cm}^2 = \pi r_0^2 * 1 \text{ cm}$$

$$r_0 = 1.5 a_0 \text{ [27, 28]}, \quad a_0 = 0.2864 \text{ nm}$$

$$d_\tau = 5.798 \times 10^{-15} \text{ cm cm}^{-1}$$

(iv) Numerous transmission electron microscopy investigations have shown that the annihilation of lattice dislocations embodied into grain boundaries is a dislocation delocalization process, and the delocalization is controlled by atom diffusion [29–32]. It was found that when the width of the dislocation core along boundary was delocalized to 100 nm, the lattice dislocation can be thought to disappear completely. Thus we obtain the relaxation time τ of dislocation disappearance [31]

$$(D_g \tau)^{1/2} = 100 \text{ nm}$$

Here the process of delocalization is probably controlled by self-diffusion in the grain. The self-diffusion coefficient D_g in α-Fe is $1.67 \exp(-61.3 \text{ kcal mol}^{-1}/kT)$ cm^2 s^{-1} [33]. Thus $\tau = 2$ s.

(v) $d_0 = 3a_0 = 8.592 \times 10^{-8}$ cm

Substituting the above parameters into Equation 13 and combining Equation 14, we obtain boron segregation on moving grain boundaries during recrystallization in α-Fe deformed 20% at 1000 °C,

$$K^{MG} = C_{gb}/C_g = 1.7$$

The above result agrees well with the experimental value of 1.6 [23].

3.3. Discussion

In the above model, the necessary conditions to produce stronger segregation of solute atoms on moving boundaries during recrystallization than on static boundaries are $U_0 > kT$ and $D_{gb} \gg V\delta$. According to these two conditions, we can expect that N, C, P and B will have perversive segregation on moving boundaries during recrystallization in steels, as does B in Fe–3% Si. The direct and/or indirect experiment results [4, 34] have already proved the strong segregation of P, C and B on moving boundaries in austenite steels.

It should be noted that the above model is simple. Further experimental and theoretical studies on this model are needed. In further studies, the different binding energies of solute atoms with static boundaries and with moving boundaries, the different structures of static boundaries and moving boundaries, and the influence of other solute atoms on the solute segregation, should be taken into consideration. Experiments [35, 36] have shown that the energy of moving boundaries and solute behaviour (such as diffusion) is considerably different from that on static boundaries. Moreover, the interactions of lattice dislocation with static and moving boundaries should be studied in more detail.

4. Conclusions

1. A model for the solute non-equilibrium segregation to grain boundaries during quenching has been suggested. The dynamic process of the segregation can be described by the following equations:

$$\frac{\partial C_B}{\partial t} = D_B \nabla^2 C_B - (R_1 D_V + R_2 D_B) \times \left(C_B C_V - \frac{C_{VB}}{K} \right)$$

$$\frac{\partial C_V}{\partial t} = D_V \nabla^2 C_V - (R_1 D_V + R_2 D_B) \times \left(C_B C_V - \frac{C_{VB}}{K} \right)$$

$$\frac{\partial C_{VB}}{\partial t} = D_{VB} \nabla^2 C_{VB} + (R_1 D_V + R_2 D_B) \times \left(C_B C_V - \frac{C_{VB}}{K} \right)$$

Applied to boron segregation to austenite grain boundaries, these theoretical calculations agree well with experimental results. The model interprets satisfactorily the different behaviour of boron segregation in γ-Fe and α-Fe. The essential conditions of quenching-induced segregation are $E_b > kT$ and $D_{VB} > D_B$.

2. The non-equilibrium segregation of solutes to moving grain boundaries during recrystallization results from the increasing width of moving boundaries,

at which a large number of lattice dislocations disappear during recrystallization. The width of recrystallized boundaries is

$$\delta = d_0 + \rho V \tau d_\tau$$

The essential conditions for non-equilibrium segregation of solute to recrystallized boundaries to occur are $U_0 > kT$ and $D_{gb} \gg V\delta$. Then the enrichment ratio on recrystallized boundaries is

$$\frac{C_{gb}}{C_g} = 1 + \frac{1}{W}(e^{\frac{U_0}{kT}} - 1)(d_0 + \rho V \tau d_\tau)$$

Acknowledgement

This research project is supported by the National Natural Science Foundation of China.

References

1. X. L. HE, Y. Y. CHU and J. J. JONAS, *Acta Metall.* **37** (1989) 147.
2. J. H. WESTBROOK and K. T. AUST, *ibid.* **11** (1963) 1151.
3. K. T. AUST, R. E. HASSEMAN, P. NIESSEN and J. H. WESTBROOK, *ibid.* **16** (1968) 291.
4. X. L. HE, M. DJAHAJI, J J. JONAS and J. JACKMAN, *Acta Metall. Mater.* **39** (1991) 2295.
5. T. TAKEYAMA, H. TAKAHASHI and S. OHNUKI, in "Grain Boundary Structure and Related Phenomena", Proceedings of Fourth Japan Institute of Metals International Symposium (Japan Institute of Metals,1986), p. 401.
6. M. B. KASEN, *Acta Metall.* **31** (1983) 489.
7. X. L. HE, Y. Y. CHU and J. J. JONAS, *ibid.* **37** (1989) 2905.
8. S. H. ZHANG, X. L. HE, Y. Y. CHU and T. KO, *Acta Metall. Sinica* **28A** (1992) 187.
9. L. KARLSSON, *Acta Metall.* **30** (1988) 25.
10. A. F. SMITH and G. B. GIBBS, *J. Met. Sci.* **2** (1968) 47.
11. J. A. HUDSON and R. S. NELSON, "Vacancies '76" (Metal Society, London 1977) p. 126.
12. P. E. BUSBY, M. E. WARGA and C. WELLS, *Trans. AIME* **197** (1953) 1463.
13. T. M. WILLIAMS, A. M. STONEHAM and D. R. HARRIES, *J. Met. Sci.* **10** (1976) 14.
14. M. J. DOYAMA, *J. Nucl. Mater.* **69, 70** (1978) 350.
15. A. F. ROWCLIFFE and R. B. NICHOLSON, *Acta Metall.* **20** (1972) 143.
16. M. A. V. CHAMPMAN and R. G. FAULKNER, *ibid.* **31** (1983) 677.
17. J. W. MILLER, *Phys. Rev.* **188** (1969) 1074.
18. W. F. JANDESKA Jr. and J. E. MORRAL, *Met. Trans.* **3** (1972) 2933.
19. R. W. BALLUFI, "Grain Boundary Structure and Kinetics" (American Society of Metals, Metals Park, Ohio, 1980) p. 297.
20. L. KARLSSON, H. NORDEN and H. ODELIUS, *Acta Metall.* **36** (1988) 1.
21. S. H. ZHANG, Ph. D Thesis, University of Science and Technology, Beijing, 1922.
22. S. H. ZHANG, X. L. HE, Y. Y. CHU and T. KO, *J. Mater. Sci.* **29** (1994).
23. S. H. ZHANG, X. L. HE and T. KO, *J. Mater. Sci.* **29** (1994).
24. J. W. CAHN, *Acta Metall.* **10** (1962) 789.
25. D. MCLEAN, "Grain Boundaries in Metals" (Oxford University Press, Oxford, 1957) p. 116.
26. K. KURZYDOLSKI, J. W. WYRZYKOWSKI and G. GARBACZ, *Phys. Met. Metall.* **65** (1988) 163.
27. S. H. ZHANG, X. L. HE and T. KO, (Submitted to *Acta Metall. Sinica*).
28. R. BULLOUGH and V. K. TEWARY, in "Dislocations in Solids, Vol. 2: Dislocations in Crystals", edited by F. R. N. Nabarro (North-Holland, 1979) p. 58.
29. M. W. GRABSKI and R. KORSKI, *Phil. Mag.* **22** (1970) 707.
30. M. W. GRABSKI and J. W. WYRZYKOWSKI, *Mater. Sci. Engng* **44** (1980) 229.
31. P. H. PUMPHERY and H. GLEITER, *Phil. Mag.* **32** (1975) 881.
32. R. A. VARIN, *Phys. Status Solidi* **52** (1979) 337.
33. E. A. BRANDES (ed) "Smithells Metals Reference Book", 6th edn, (Butterworth, 1983) p. 13.
34. T. ABE, K. TSAKADA, H. TAGAWA and I. KOZASSA, *Tetsu-to-Hagane (Iron and Steel)* **74** (1988) 2201 (in Japanese).
35. M. HILLERT and G. R. PURDY, *Acta Metall.* **26** (1978) 333.
36. K. SMIDODA, W. GOTTSCHALK and H. GLEITER, *ibid.* **26** (1978) 1833.
37. D. A. SMITH, *Ultramicroscopy* **29** (1989) 1.

Received 30 March
and accepted 19 October 1993